Isothermal Crystallization and Melting Behavior of 2-Methyl-1,3-propanediol Substituted Sulfonated Poly(ethylene terephthalate) Copolyesters

Bin Chen, Lixia Gu

State Key Laboratory for Modification of Chemical Fiber and Polymer Materials, College of Materials Science and Engineering, Donghua University, Shanghai 201620, People's Republic of China

Received 21 September 2009; accepted 19 January 2010
DOI 10.1002/app.32119
Published online 13 April 2010 in Wiley InterScience (www.interscience.wiley.com).

ABSTRACT: Poly(ethylene terephthalate) copolyesters (abbreviated as MCDP) containing 2-methyl-1,3-propanediol (MPD) and sodium-5-sulfo-bis-(hydroxyethyl)-isophthalate (SIP) units were synthesized through a direct polycondensation reaction. Chemical compositions of the copolyesters were determined by ^{1}H- and ^{13}C- NMR spectroscopy, respectively. Thermal properties and isothermal crystallization behavior were characterized using DSC analysis. Results exhibited that the crystallization rate of MCDP copolyesters was depressed with increasing MPD content. The equilibrium melting temperature of MCDP copolyesters showed a marked decrease when the composition of MPD increased, indicating the incorporation of MPD units lead to less perfect crystals. The crystal structure was investigated via using WAXD patterns. It was confirmed that MPD and SIP can not enter into the crystal region. The crystal morphology observed by using POM clearly showed that the presence of MPD units depressed the crystallization ability of MCDP copolyesters. © 2010 Wiley Periodicals, Inc. J Appl Polym Sci 117: 2454–2463, 2010

Key words: copolyester; thermal properties; isothermal crystallization

INTRODUCTION

Poly(ethylene terephthalate) (PET) has many outstanding properties for textile and industrial fiber applications, but it is difficult to dye because of its high crystallinity, marked hydrophobicity, and lack of chemically active groups.[1–5] It is well known that copolymerization of polyesters with ionic groups constitutes a very effective method to improve both chemical and physical properties of the polymer.[6,7] Development of cationic dyeable polyester (CDP) fibers has shown a success in solving a problem of dullness of shades in regular PET fibers, because CDP fibers contain 1–3 mol % sulfonated units ($-SO_3^-Na^+$), which can get bright and lively colors by dyeing with cationic dyes. Thus CDP are known as the most successful modified PET for improving dyeability of PET fibers, but it also exhibits limitations such as higher melt viscosity, poorer spinnablity, and lower strength. These disadvantages are generally attributed to the formation of ionic aggregates within the organic matrix which act as thermo-reversible cross-links[8,9] and effectively retard the translational mobility of the chains. More importantly, the dyeing conditions for CDP fibers still require high temperature as well as high pressure because of the high crystallinity. To overcome the shortcoming and further develop the textiles properties of CDP, we added 2-methyl-1,3-propanediol (MPD) into the esterification process of CDP, and finally synthesized a novel cationic dyeable copolyester (MCDP). In a related study, Lewis and Spruiell[10] found that MPD can reduce crystallization rate of modified PET effectively. Suh et al.[11] revealed that the modified PET containing MPD has good spinnability and possesses high commercial values. However, no prior studies of adding MPD into CDP were found.

In this work, we found that the dyeability of MCDP fibers was much better than that of CDP fibers with same SIP content, and MCDP fibers can even be possibly dyed to deep color under normal temperature and pressure conditions. All these property changes might be related to the incorporation of MPD units into polymer backbone, which leads to an irregular chain structure and thereby influences regular chain packing for crystallization. Therefore, this article will discuss the effect of the addition of MPD on the crystallization behavior of MCDP copolyester. Relevant to these aspects, the melting behavior and the crystal structure of MCDP copolyester have also been investigated.

Correspondence to: L. Gu (gulx@dhu.edu.cn).

TABLE I
Sample Code, Feed Ratio, Composition Calculated from NMR and Intrinsic Viscosity of MCDP Copolyesters

Sample	Feed ratio[a]		Relative amounts from ^{1}H NMR		Relative amounts from ^{13}C NMR		Intrinsic viscosity (dL/g)	DEG content (mol %)
	EG/MPD	PTA/SIP	EG/MPD	PTA/SIP	EG/MPD	PTA/SIP		
CDP	100/0	97/3	100/0	97.08/2.92	100/0	97.15/2.85	0.512	3.76
MCDP 2	98/2	97/3	96.86/3.14	97.00/3.00	96.91/3.09	97.09/2.91	0.512	3.55
MCDP 6	94/6	97/3	92.73/7.27	97.16/2.84	93.12/6.88	97.08/2.92	0.520	3.92
MCDP 10	90/10	97/3	87.64/12.36	97.08/2.92	87.95/12.05	97.21/2.79	0.486	3.88

[a] Molar ratio of EG and MPD monomers fed in polymerization.

EXPERIMENTAL

Materials

MCDP copolyester was synthesized by using purified terephthalate acid (PTA; Yizheng Chemical Fibers, China), ethylene glycol (EG; Yangzi Petrochemical, China), 2-methyl-1,3-propanediol (MPD; Lyondell Chemical, USA) and sodium-5-sulfo-bis-(hydroxyethyl)-isophthalate (SIP; Yangzhou Huitong, China).

PET homopolymer was purchased from Yizheng Chemical Fibers, China. The intrinsic viscosity is 0.675 dL/g.

Synthesis of copolyesters

MCDP copolyester was prepared according to direct polycondensation method commonly used for polyester synthesis. The esterification of PTA, EG, and MPD (feed molar ratio: diacids/diols = 1/1.4) was run at 180 $\sim$ 240°C for 1.5 $\sim$ 2 h in the presence of antimony triacetate as catalyst, water being removed by distillation at atmospheric pressure. Then the SIP (feed molar ratio: SIP/PTA = 3/97) was added to esterification product before the subsequent condensation reaction, which was carried out at 260 $\sim$ 275°C for 1 $\sim$ 1.5 h under a vacuum of less than 1 torr. Finally, MCDP copolyester was obtained.

The four copolyesters with various MPD/EG feed molar ratios (0/100, 2/98, 6/94, 10/90) were prepared, designated as CDP, MCDP2, MCDP6, and MCDP10, respectively. The intrinsic viscosities of these copolyesters ranged between 0.486–0.52 dL/g (Table I), which were measured at 25°C using phenol/tetrachloroethane (3 : 2, w/w) as a mixing solvent.

Measurement and characterization

^{1}H NMR and ^{13}C NMR spectra were recorded using a Bruker Avance400 NMR spectrometer. MCDP copolyesters were dissolved in a mixture of deuterated chloroform/deuterated trifluoroacetic acid (3 : 1, v/v), and tetramethylsilane was used as an internal standard.

Thermal analysis was performed under nitrogen using a TA 2910 Modulated DSC. The samples were melted for 5 min at melt-annealing temperature about 30°C above the corresponding melting temperature, and then quenched into liquid nitrogen as quickly as possible. The heating scan was started from 40°C at a heating rate of 20°C min^{-1} to the corresponding melt-annealing temperature, and then kept for a period of 5 min. After that, the cooling run was carried out at a cooling rate of 20°C min^{-1}.

Isothermal crystallization and subsequent melting behavior were analyzed via using a Perkin Elmer Diamond DSC. Each sample was used only once and all the runs were carried out under nitrogen atmosphere to prevent thermal degradation. The sample with weight of 5–6 mg was started from 40°C at a heating rate of 50°C min^{-1} to a desired melt-annealing temperature and then kept for 5 min. After this period, each sample was rapidly cooled from melt-annealing temperature to a selected crystallization temperature, where it was held for the completion of the crystallization process, which was confirmed by reaching a point where no obvious change in the heat flow as a function of time was further observed. Finally, the sample was heated to 300°C at a rate of 20°C min^{-1} for studying the melting behaviors.

Wide angle X-ray diffraction (WAXD) was employed to determine the crystal structure changes and apparent crystallinity of MCDP copolyesters. The samples were firstly crystallized completely under vacuum at 120°C for 24 h, and then these samples in powder form were measured at room temperature on a X-ray diffractometer (D/MAX-rB, Rigaku), using Ni-filtered Cu Kα radiation as a radiation source.

Optical micrographs were obtained with polarizing optical microscopy (POM, BX51 Olympus). A thin sample piece was sandwiched between two glass coverslips and placed on the digital hotplate under nitrogen. The hotplate was rapidly heated to 300°C and kept for 5 min, the melt was gently

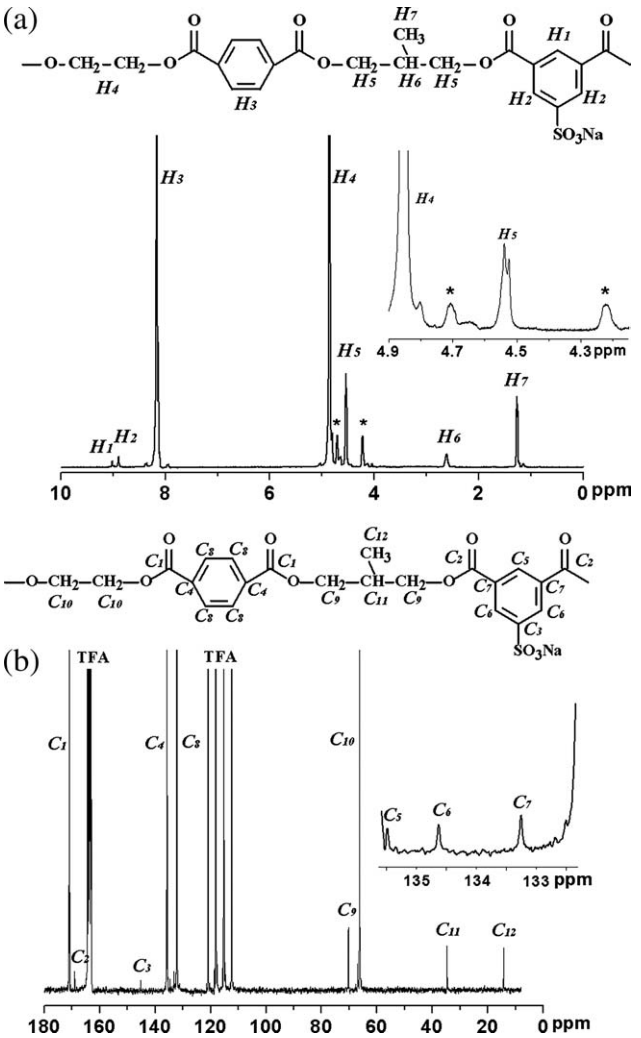

Figure 1 ^{1}H-NMR (a) and ^{13}C-NMR (b) spectra of MCDP10. The asterisk in ^{1}H-NMR denotes DEG content. TFA in ^{13}C-NMR represents deuterated trifluoroacteic acid.

pressed to achieve a uniform thickness, then rapidly cooled to a desired crystallization temperature, where it was 75°C below the equilibrium melting temperature, and kept for 5 min. The images were recorded by the CCD camera.

RESULTS AND DISCUSSION

Composition of MCDP copolyesters

The chemical structure of the copolyester was ascertained by NMR spectroscopy. ^{1}H-NMR and ^{13}C-NMR spectra revealed clear differences in the chemical shifts of signals that arose from PTA, EG, SIP, and MPD units. The typical ^{1}H-NMR and ^{13}C-NMR spectra of MCDP10 are shown in Figure 1, together with the chemical shift assignments. Similar spectra were obtained for other MCDP copolyesters. In all cases, the spectra were found consistent with the expected structures. The inset figure of ^{1}H-NMR spectrum in Figure 1(a) shows that the H_5 proton has two signals due to the different sequence of PTA and SIP units centered at MPD units. Similar behavior also can be observed from the H_4 proton, indicating the different sequence of PTA and SIP units linked to EG units. The compositions of the prepared copolyesters were determined from the relative integration areas of different resonances peaks in ^{1}H-NMR and ^{13}C-NMR spectra,[12] respectively, using the following equations:

$$\frac{\mathrm{EG}}{\mathrm{MPD}} = \frac{\mathrm{H_4}}{4\mathrm{H_6}} \quad \text{or} \quad \frac{\mathrm{EG}}{\mathrm{MPD}} = \frac{\mathrm{C_{10}}}{2\mathrm{C_{11}}} \tag{1}$$

$$\frac{\mathrm{PTA}}{\mathrm{SIP}} = \frac{\mathrm{H_3}}{2\mathrm{H_2}} \quad \text{or} \quad \frac{\mathrm{PTA}}{\mathrm{SIP}} = \frac{\mathrm{C_1}}{\mathrm{C_2}} \tag{2}$$

The calculated values of EG/MPD and PTA/SIP of all copolyesters are given in Table I. The results calculated from ^{1}H-NMR are in good agreement with those calculated by ^{13}C-NMR. However, based on NMR results the prepared copolyesters are slighter rich in MPD units when compared with the given feed composition ratios. This result could be ascribed to the higher boiling temperature of MPD, resulting in more MPD staying in the system during the polycondensation process, which finally increased the MPD content in MCDP copolyesters.[13,14]

It is well known that in the polymerization of PET, under certain conditions, the EG can undergo a hydration reaction to produce diethylene glycol (DEG), which may polymerize with the terephtalate moiety. From the inset figure of ^{1}H-NMR spectrum, it can be found that a small amount of DEG existed in the molecular chain (marked as asterisk in ^{1}H-NMR).[15] The amount of this component was analyzed and reported in Table I. The DEG contents in different samples were very similar; around 3.55–3.92 mol %, as the DEG formation was strongly dependent on the adopted polymerization procedure.[15] Thus, the effect of the small amount DEG on the properties of MCDP copolyesters should be equal. Moreover, Jackson and Longman[16] has proven that at a level of DEG content of 2–5 mol % and crystallization temperatures of 140–220°C, there should be no significant effect of DEG on crystallization ability of polyester. Therefore, the DEG content will not be considered as an important factor for the following discussion.

Thermal properties of MCDP copolyesters

The thermal behavior of a polymer is affected by its previous thermal history and, therefore, each sample was kept under a melt-annealing temperature of

TABLE II
Thermal Properties of MCDP Copolyesters

	DSC heating scan					DSC cooling scan	
Sample	T_g (°C)	T_{cc} (°C)	ΔH_{cc} (J/g)	T_m (°C)	ΔH_m (J/g)	T_{mc} (°C)	ΔH_{mc} (J/g)
CDP	79.5	175.2	27.4	241.3	28.7	188.8	30.7
MCDP2	78.6	180.2	18.3	235.6	19.1	175.8	21.6
MCDP6	76.3	186.3	1.9	225.5	2.2	165.2	8.0
MCDP10	74.5	187.7	1.1	212.2	1.2	150.9	2.7

30°C above the corresponding melting temperature for 5 min, and then quenched into the liquid nitrogen as quickly as possible, to completely prevent crystallization and obtain polymers in completely amorphous status. Then the so-treated samples were heated from 40°C at a rate of 20°C min^{-1} to the corresponding melt-annealing temperature (heating run), and kept there for a melt-annealing period of 5 min. After this period, each sample was cooled from the melt-annealing temperature to 40°C at a cooling rate of 20°C min^{-1} (cooling run). All the results are summarized in Table II.

As expected, the T_g of CDP and MCDP copolyesters gradually moved to a lower temperature when the amount of MPD units increased, indicating the addition of MPD units enhanced the chain irregularity and increased the free volume, and therefore less energy was required for molecular motion and rearrangement. In addition, all of MCDP copolyesters exhibited a single T_g value rather than two or more T_g values, implying that co-units placement in these copolyesters was essentially random.

Generally, the effect of co-units on the crystallization behavior can be characterized by a cold-crystallization temperature (T_{cc}) and melt-crystallization (T_{mc}) of MCDP copolyesters, with higher T_{cc} or lower T_{mc} corresponding to lower crystallization rate. As shown in Table II, it is evident that CDP had the highest T_{cc} and the lowest T_{mc} compared with those of MCDP copolyesters. The increasing amount of MPD units lead to an increase of T_{cc} and a reduction of T_{mc}, suggesting that the crystallization ability of MCDP copolyesters was strongly affected by the quantity of the MPD units, which probably played a negative role in the crystallization process.

Traditional DSC measurements provide a summation of endothermic and exothermic process, which are often confusing and sometimes misleading. Thus modulated dsc (MDSC) was used to characterize the crystallization behavior in this study. The total heat flow obtained from MDSC is composed of reserving heat flow and nonreserving heat flow. For all the samples, the crystallization and melting enthalpy values measured from the reserving and nonreserving heat flow were very comparable, confirming that the starting state of samples was amorphous. The melting peak could be detected in both of the total and reversing heat flows (Fig. 2(a,b)). It was observed that the increasing of MPD amount lead to a reduction of the melting temperature (T_m) and a widening of the melting peak, indicating that the incorporation of MPD resulted less perfect crystals. In the nonreserving heat flow [Fig. 2(c)], it shows two exothermic peaks. One exothermic peak at low temperature was attributed to the cold-crystallization process which also can be observed in total heat flow. The other crystallization peak at high temperature was attributed to the recrystallization process. With increasing the MPD amounts, the nonreserving curves showed that both of the two exothermic peaks became weaker and weaker, suggesting that the crystallization ability of MCDP copolyesters were depressed by introducing MPD units into the molecular chain.

Isothermal crystallization

The crystallization process was studied by DSC in isothermal conditions, and the neat PET was also included for comparison. Figure 3 illustrates the relative crystallinity $\theta(t)$ versus time t plots for the MCDP6 polymer at various crystallization temperatures. Evidently, within the temperature range studied, the time for reaching the completed crystallization increased with the increasing of crystallization temperature. Similar behavior was observed for other samples. From these curves, the half-time of crystallization ($t_{0.5}$) can be directly determined, which is defined as the elapsed time from the onset of crystallization to the point where the half-completed crystallization is reached. Figure 4 shows the plot of the reciprocal crystallization time ($1/t_{0.5}$) versus the undercooling ($\Delta T = T_m^0 - T_c$), to evaluate the crystallization rate of different polymers in comparable crystallization conditions.[17,18] For all samples, the plots indicate that the $1/t_{0.5}$ increased with increasing ΔT. This may be explained based on the fact that the number of athermal nuclei became stable at a lower crystallization temperature.[19] Comparing the $1/t_{0.5}$ of PET to that of CDP at a given undercooling ΔT, it is evident that the crystallization rate of CDP was lower due to the presence of SIP units. Concerning CDP and MCDP copolyesters, it can be observed that the crystallization rate of MCDP copolyesters at

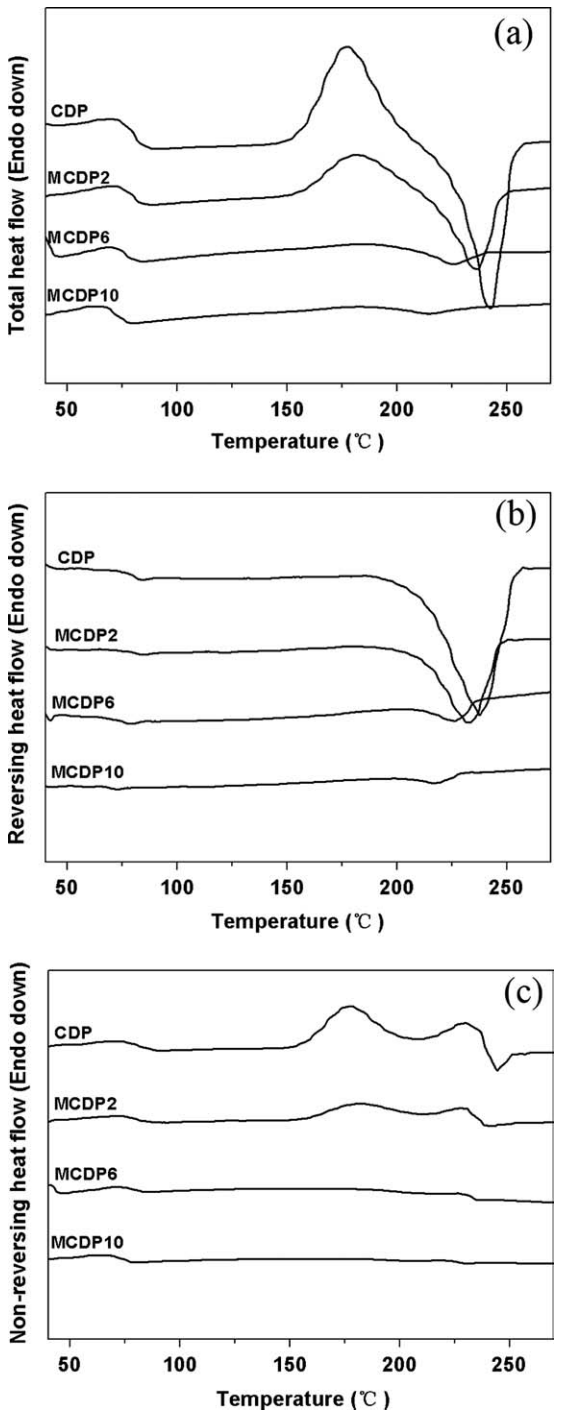

Figure 2 DSC curves (heating scan) of MCDP copolyesters after quenching in liquid nitrogen. (a) Total heat flow; (b) Reversing heat flow; (c) Nonreversing heat flow.

a given undercooling ΔT were further decreased with increasing MPD concentration, suggesting that MPD units played a negative effect on the regular chain packing.

In this study, Avrami equation[20–22] was used to analyze the isothermal crystallization process of these copolyesters:

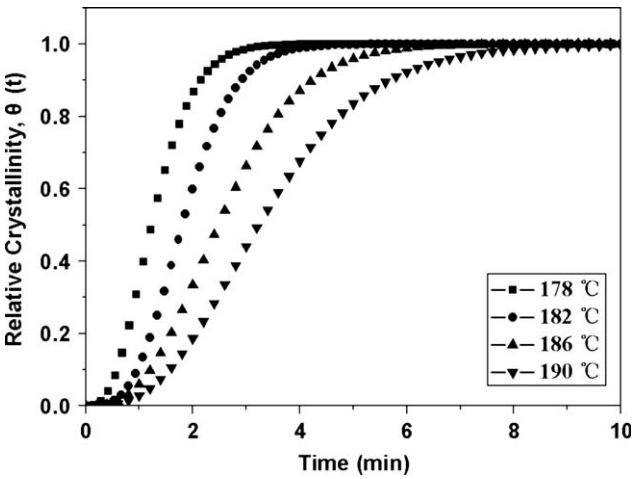

Figure 3 Relative crystallinity versus crystallization time for MCDP6 copolyester.

$$1 - \theta_{(t)} = \exp(-kt^n) \tag{3}$$

$$\ln[-\ln(1 - \theta_{(t)})] = n \ln t + \ln k \tag{4}$$

where n is the Avrami exponent and k is Avrami rate constant. According to the equation a plot of $\ln[-\ln(1 - \theta_{(t)})]$ as a function of lnt should yield a straight line with slope equal to n, and y-intercept equal to $\ln k$. Figure 5 shows the plots of $\ln[-\ln(1 - \theta_{(t)})]$ versus $\ln t$ according to eq. (4) for the isothermal crystallization of MCDP6. Other samples have the similar quality plots with MCDP6. It is usual to distinguish the crystallization behavior at the linear stage, i.e., before the kinetic curve deviates markedly from the theoretical isotherms as well as the primary crystallization and the secondary crystallization

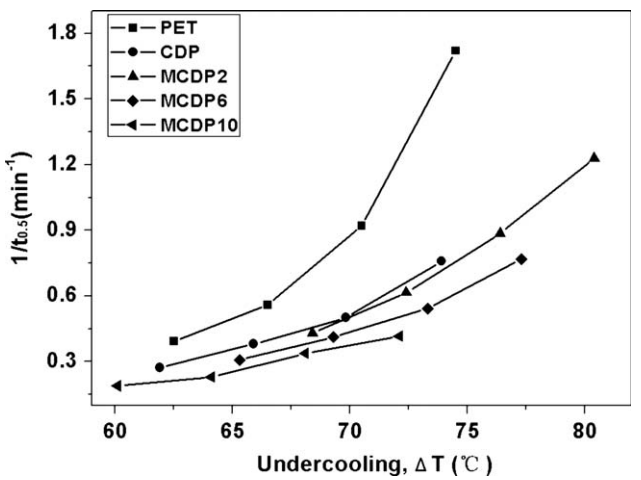

Figure 4 Reciprocal half-time of crystallization $1/t_{0.5}$ as a function of degree of undercooling.

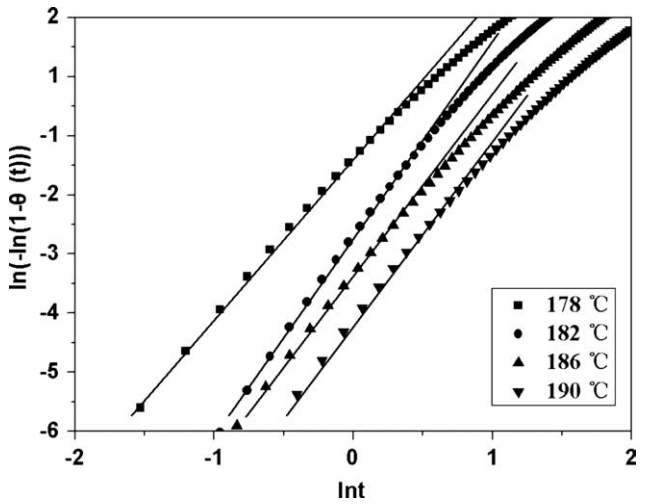

Figure 5 Avrami plots for MCDP6 copolyester at different crystallization temperature.

occur at the nonlinear stage. The primary crystallization consists of outward growth of lamellar stacks until impingement and the secondary crystallization, which may overlap the primary crystallization and fill the spherulites of interstices.[23,24] In this work, we focused only on the primary crystallization. The results of the isothermal Avrami analysis are summarized in Table III. The n values found in the case of neat PET were in the vicinity of 2.4 ± 0.1. This probably corresponded to a three-dimensional growth with a combination of thermal and athermal nucleation (resulting in the fractional values of n observed). These values are in good agreement with corresponding literature data, reported by Lu and Hay.[25] On the other hand, it was observed that the n values of CDP and MCDP copolyesters were very similar; about 2.8–3.1, indicating that the growth type also should be a three-dimensional growth. Indeed, all the samples exhibited a spherulites-like crystal based on the observation of the crystal morphology, seen in Figure 10. Furthermore, the n values of CDP and MCDP copolyesters are different from that of neat PET, suggesting that the addition of SIP and MPD units into PET structure induced a change in crystallization mechanism. In addition, it could be presumed that MPD and SIP units play a very similar role in affecting the chain packing for crystallization because of their irregular molecular chain structures.

From the kinetic data shown in Table III, k is very sensitive to changes in the crystallization temperature, deceasing with increasing crystallization temperature, similar to the case of $t_{0.5}$ previously shown. Indeed, The Avrami rate constant k also can be determined from the $t_{0.5}$, according to the equation:

TABLE III
Isothermal Crystallization Kinetics Parameters

Sample	T_c (°C)	n	k (min^{-1})	$k_{0.5}$ (min^{-1})
PET	206	2.3	2.36	2.43
	210	2.5	0.548	0.564
	214	2.5	0.156	0.166
	218	2.4	0.0706	0.0747
CDP	198	2.8	0.339	0.319
	202	2.8	0.0891	0.0902
	206	2.9	0.0435	0.0415
	210	3.0	0.0162	0.0149
MCDP2	182	2.9	1.28	1.25
	186	2.9	0.461	0.49
	190	2.8	0.185	0.178
	194	3.0	0.0239	0.0656
MCDP6	178	2.8	0.329	0.331
	182	3.1	0.0985	0.103
	186	3.0	0.0344	0.0495
	190	3.0	0.019	0.019
MCDP10	176	2.9	0.062	0.0635
	180	3.1	0.0232	0.0227
	184	3.0	0.00889	0.00885
	188	3.1	0.00421	0.00386

$$k_{0.5} = \frac{\ln 2}{t_{0.5}^n} \tag{5}$$

The calculated rate constant values $k_{0.5}$ are listed for comparison in Table III. Obviously, the values determined from the fitting of the experimental data k were consistent with that determined from the calculated $k_{0.5}$.

Melting behavior and equilibrium melting temperature

Every sample was processed to successive DSC melting endotherms after complete isothermal

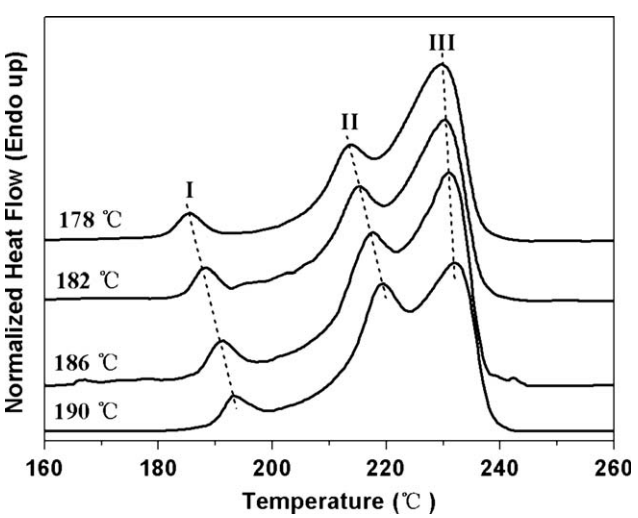

Figure 6 Melting behaviors of MCDP6 after isothermal crystallization.

TABLE IV
Melting Temperature after Isothermal Crystallization

Sample	T_c (°C)	T_m I (°C)	T_m II (°C)	T_m III (°C)	T_m^0 (°C)
PET	206	220.0	245.8	262.3	280.5
	210	223.5	247.7	262.3	
	214	227.6	249.7	262.4	
	218	232.3	251.5	262.8	
CDP	198	206.3	230.3	246.0	271.9
	202	210.8	232.6	246.7	
	206	215.2	234.9	246.9	
	210	218.5	237.0	247.0	
MCDP2	182	188.9	217.7	235.1	262.4
	186	194.1	220.2	236.0	
	190	197.3	222.2	236.1	
	194	201.1	224.5	236.2	
MCDP6	178	185.5	213.5	229.8	255.3
	182	188.3	215.4	230.1	
	186	191.2	217.7	230.8	
	190	193.3	219.9	230.9	
MCDP10	176	184.7	208.9	221.5	248.1
	180	186.9	211.1	221.3	
	184	190.1	213.1	221.2	
	188	192.3	215.5	222.6	

crystallization from the melt state at various crystallization temperatures. It was found that all the copolyesters exhibited the triple-peak melting endotherms. Figure 6 shows the DSC melt endotherms of MCDP6. The peaks are labeled as I, II, and III for low-, middle-, high-temperature melting endotherms, respectively. Many investigators attributed the peak I to the melting subsidiary lamellae (from the secondary crystallization), the peak II to the melting of the dominant lamellae, and the peak III to the recrystallization.[26,27]

The corresponding temperature values of the triple melting peaks are listed in Table IV. Based on the results, it can be seen that the peak I and peak II both shifted to the higher temperature as the isothermal crystallization temperature increased. However, the peak III did not shift significantly with the increasing crystallization temperature. This behavior demonstrates that more perfect crystals formed as the crystallization temperature increased. Assuming the melting enthalpy of peak II is only attributed to the crystals formed during the isothermal crystallization process, then the equilibrium melting temperature (T_m^0) can be estimated by the Hoffman-Weeks theory[28] by using corresponding temperature value of the peak II. As seen in Figure 7, all the Hoffman-Weeks plots of different copolyesters illustrate good linearity. The T_m^0 of neat PET was 280.5°C, which is consistent with 280°C reported in the literature for neat PET.[29] In terms of MCDP copolyesters, the T_m^0 gradually decreased with increasing MPD content. This result indicates that the incorporation of MPD units inhibited the crystallization ability of MCDP copolyesters, leading to formation of less perfect crystals.

The equilibrium melting temperature was also examined via using Flory's[30] and Baur's equation,[31] which is derived assuming that if one co-unit crystallizes, the other co-units are completely excluded from the crystals. The curves drawn in Figure 8 were calculated according to Flory's [eq. (1)] and Baur's [eq. (2)] equations:

$$\frac{1}{T_m} = \frac{1}{T_m^0} - \frac{R}{\Delta H_m^0} \ln x \tag{6}$$

$$\frac{1}{T_m} = \frac{1}{T_m^0} - \frac{R}{\Delta H_m^0} (\ln x - \xi^{-1}) \tag{7}$$

where T_m and T_m^0 are the equilibrium melting temperatures of the copolyesters and pure

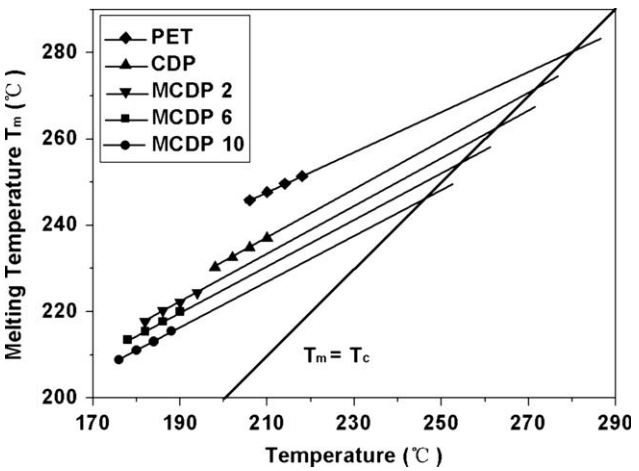

Figure 7 Hoffman-Weeks plots for samples after isothermal crystallization.

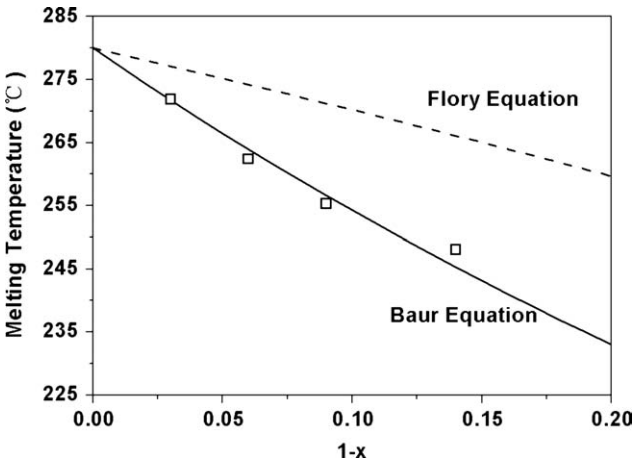

Figure 8 Composition dependence of equilibrium melting temperature (T_m^0) for MCDP copolyesters. Dashed lines and solid lines represent the Flory's equation and Baur's equation, respectively.

homopolymer (PET, $T_m^0 = 280°C$[32]), respectively; x is the molar content of the crystallizable monomer, and ΔH_m^0 is the melting enthalpy per mole of repeating unit of the crystallizable polymer (PET, $\Delta H_m^0 = 26.9$ kJ/mol[32]), and R is the gas constant. In eq. (7), $\xi = 1/[2x(1 - x)]$ represents the average length of crystallizing sequence.

Figure 8 shows that the Baur's equation provided a much better fit to the experimental results than the Flory's equation. It can be supposed that both MPD and SIP units are rejected from the crystal region. In addition, on the basis of the assumptions of the Baur's equation, it is also revealed that the average length of the crystallizing sequences decreased along the series with MPD content in this study. Thus, the equilibrium melting temperature was decreased as MPD content was increased.

Crystal structure of MCDP copolyesters

To further investigate the crystal structure of different MCDP copolyesters, the WAXD analysis was used, and the WAXD patterns are shown in Figure 9. Compared with WAXD patterns of PET, it is found that there was no significant positional change of the diffraction peaks among PET, CDP, and MCDP copolyesters. The diffraction peaks of triclinic PET at 2θ of 17.1, 22.5, 25.9, and 28.1°, corresponding to overlapping ($0\bar{1}1$, 010), overlapping ($\bar{1}11$, $1\bar{1}0$), (100) and ($1\bar{1}1$) reflection planes respectively,[33,34] suggesting that the only one crystal structure of these MCDP copolyesters was triclinic system in the same manner as of PET. In other words, it is also evident that only the PET segments in MCDP copolyester were able to crystallize. The results appear to further support the claim that MPD and SIP units were excluded from the crystal region.

Figure 10 shows the crystalline morphologies of various samples. To compare the crystallization rate, the samples were crystallized at the same undercooling ($\Delta T = 75°C$). Generally, it can be observed that all the samples could grow spherulites from melt. Furthermore, the neat PET showed largest size of spherulites, suggesting the crystallization rate of PET was highest due to its regular molecular structure. For CDP and MCDP copolyesters, it can be noticed that the size of spherulites gradually decreased as MPD content increased, indicating the crystallization rate were reduced because MPD acts as obstacles to inhibit the regular packing of polymer chains.

CONCLUSIONS

A series of novel MPD substituted sulfonated PET copolyesters in different chemical compositions were synthesized. The MPD contents in final copolyesters were slightly higher when compared with the given feed composition ratios due to the differences in the glycols vapor pressures. The thermal property study and isothermal crystallization analysis revealed that the incorporation of MPD units led to an irregular

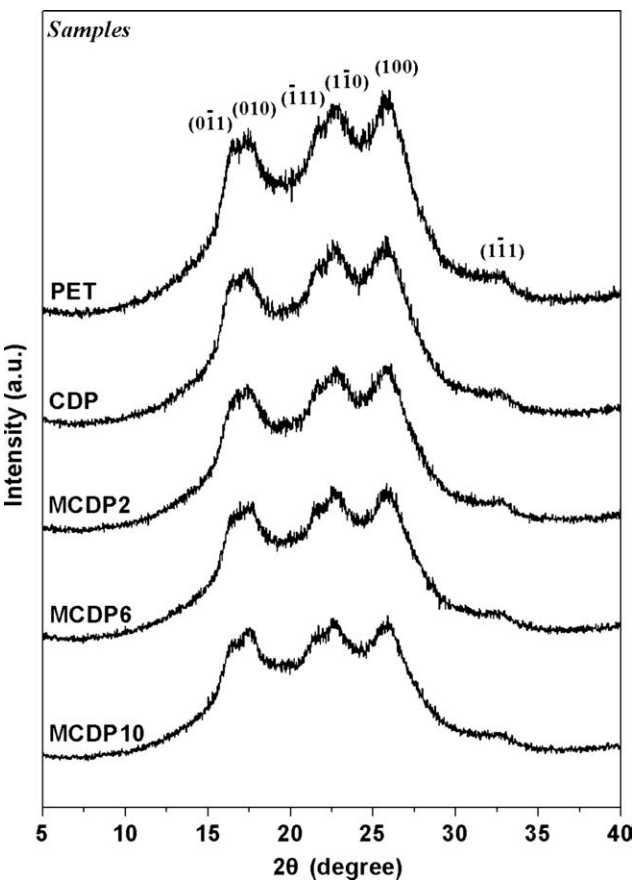

Figure 9 WAXD diffractograms for MCDP copolyesters after isothermal crystallization at 120°C for 24 h.

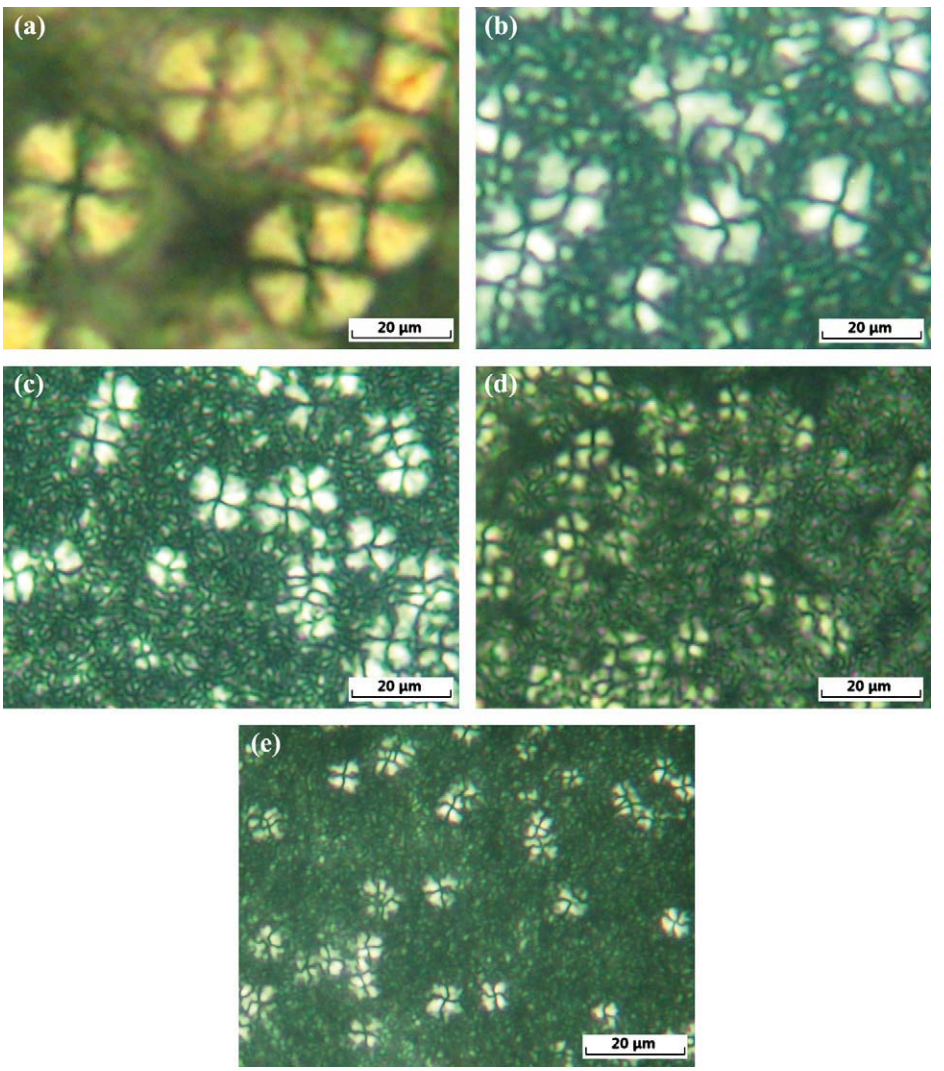

Figure 10 POM pictures of (a) neat PET, (b) CDP, (c) MCDP2, (d) MCDP6, and (e) MCDP10 isothermally crystallization at the same undercooling. [Color figure can be viewed in the online issue, which is available at www.interscience.wiley.com.]

chain structure and thereby inhibited regular chain packing for crystallization. Moreover, based on the isothermal crystallization kinetics it might be induced that MPD units played a very negative effect on the crystallization. After isothermal crystallization, multiple melting endotherms were obtained for all samples. The equilibrium melting temperature appeared to be well correlated to the composition by the Baur's equation, indicating an exclusion crystallization behavior. Only PET segments were able to enter into the crystal lattice. WAXD patterns also confirmed that MCDP copolyesters had the same crystal structure to the neat PET. The crystal morphology demonstrated that the crystallization rate was depressed with increasing MPD content. According to the results of this study, it is concluded that the incorporation of MPD can be used to modify the crystallization properties of CDP copolyester, and thus it would be necessary to further study the structure and crystallization effects on the fiber properties of MCDP in the future.

The authors acknowledge the financial support from National Science and Technology Support Program: Preparation and application of the super soft and easily dyeable polyester fiber (No. 2009BAE75B02, China), and the technique assistance from Professor Gang Sun's research group in University of California, Davis (CA, USA).

Reference

1. Eisenbach, C. D.; Stadler, E.; Enkelmann, V. Macromol Chem Phys 1995, 196, 833.
2. Bier, P.; Binsak, R.; Vernaleken, H.; Rempel, D. Angew Makromol Chem 1977, 65, 1.
3. Bouma, K.; Regelink, M.; Gaymans, R. J. J Appl Polym Sci 2001, 80, 2676.
4. Tang, S.; Xin, Z. Polymer 2009, 50, 1054.
5. Eisenberg, A.; Hird, B.; Moore, R. B. Macromolecules 1990, 23, 4098.

6. Li, X. G.; Lu, Q. F.; Huang, M. R. Small 2008, 8, 1201.
7. Li, X. G.; Feng, H.; Huang, M. R. Chem Eur J 2009, 15, 4573.
8. Hong, Z. Appl Polym Sci 1987, 34, 1353.
9. Timm, D. A.; Hsieh, Y. L. J Polym Sci: Polym Phys Ed 1993, 31, 1873.
10. Lewis, C. L.; Spruiell, J. E. J Appl Polym Sci 2006, 100, 2592.
11. Suh, J.; Spruiell, J. E.; Schwartz, S. J Appl Polym Sci 2003, 88, 2598.
12. Li, X. G.; Huang, M. R.; Guan, G. H.; Sun, T. Angew Makromol Chem 1995, 227, 69.
13. Wei, G. F.; Wang, L. Y.; Chen, G. K.; Gu, L. X. J Appl Polym Sci 2006, 100, 1511.
14. Lee, J. W.; Lee, S. W.; Lee, B.; Ree, M. Macromol Chem Phys 2001, 202, 3072.
15. Finelli, L.; Fiorini, M.; Siracusa, V.; Lotti, N.; Munari, A. J Appl Polym Sci 2004, 92, 186.
16. Jackson, J. B.; Longman, G. W. Polymer 1969, 10, 873.
17. Mandelkern, L. Comprehensive Polymer Science; Pergamon Press: Oxford, 1989; Vol. 2.
18. Wunderlich, B. Macromolecular Physics. Crystal Nucleation, Growth, Annealing; Academic: New York, 1976; Vol. 2.
19. Supaphol, P. Thermochim Acta 2001, 370, 37.
20. Avrami, M. J Chem Phys 1939, 7, 1103.
21. Avrami, M. J Chem Phys 1940, 8, 212.
22. Avrami, M. J Chem Phys 1941, 9, 177.
23. Hillier, I. H. J Polym Sci (A) 1965, 3, 3067.
24. Price, F. P. J Polym Sci (A) 1965, 3, 3079.
25. Lu, X. F.; Hay, J. N. Polymer 2001, 42, 9423.
26. Zhou, C.; Clough, S. B. Polym Eng Sci 1988, 28, 65.
27. Wang, Z. G.; Hsiao, B. S.; Sauer, B. B.; Kampert, W. G. Polymer 1999, 40, 4615.
28. Hoffman, J. D.; Weeks, J. J. J Res Narl Bur Stand A 1962, 66, 13.
29. Phillips, P. J.; Tseng, H. T. Macromolecules 1989, 22, 1649.
30. Flory, P. J. J Chem Phys 1947, 15, 684.
31. Baur, V. H. Makromol Chem 1966, 98, 297.
32. Wendling, J.; Suter, U. W. Macromolecules 1998, 31, 2516.
33. Wang, Z. G.; Hsiao, B. S.; Fu, B. X.; Liu, L.; Yeh, F.; Sauer, B. B. Polymer 2000, 41, 1791.
34. Wang, B.; Li, C. Y.; Hanzlicek, J.; Cheng, S. Z. D.; Geil, P. H.; Grebowicz, J. Polymer 2001, 42, 7171.